An Oil Outflow Model for Tanker Collisions and Groundings

Giel van de Wiel[a], J. René van Dorp[b,*],

[a] *Department of Electrical Engineering, Mathematics and Computer Science,*
The Delft University of Technology, The Netherlands
[b] *Department of Engineering Management and Systems Engineering,*
The George Washington University, USA.

Abstract: In this paper we have developed an oil outflow model for collision and grounding accidents of tankers. The collision model explicitly links input variables such as tanker hull design (single or double), displacement and speed, striking vessel displacement and speed, and the interaction angle of both vessels to output variables: longitudinal and transversal damage extents of the tanker. Overlaying these damage extents on the tank vessel's design yields an oil outflow volume totaling the capacity of the damaged tank compartments. A similar model is developed for grounding accidents. A total of 80,000 simulation accident scenarios described in the National Research Council SR259 report published in 2001 served as the joint data set of input and output variables used in this "linking" process. The oil outflow model herein was designed keeping computational efficiency in mind to allow for its integration with a maritime transportation system (MTS) simulation. We shall demonstrate the use of the oil outflow model as a final analysis layer to evaluate double-hull effectiveness in a geographic context of an MTS simulation model developed for the oil transportation routes traversing the environmentally sensitive San Juan Islands area in Washington State.

Keywords: Kinetic energy; Polynomial and logistic regression; Maritime transportation simulation.

1. Introduction

Maritime transportation plays an irreplaceable and ever-growing role in the global economy, taking up 96% of the world's global freight in terms of weight (Rodrigue et al., 2006). In 2006, sea borne trade grew 5.5% to 30,686 billion ton-miles. Of goods loaded, crude oil and petroleum products represented 36% (UNCTAD, 2007). Of course, transportation of goods by sea carries the risk of marine accidents, i.e. an event where a ship adversely interacts with its environment, possibly causing damage to either the ship, the environment, or both. When oil tankers are involved in accidents, a

---

* Corresponding author. E-mail: dorpjr@gwu.edu, Tel.: +1 202 994 6638; fax:+1 202 994 0245.

typical consequence of resulting damage is the release of crude oil or petroleum products into the sea. Recall the oil tanker Exxon Valdez running aground on March 24, 1989, shortly after leaving the Valdez oil terminal in Alaska, spilling 36,000 metric tons of crude oil into Prince William Sound and beyond, in total affecting 1,500 miles of coastline. One lesson of the Exxon Valdez accident is that sea borne oil spills from tanker ships have the potential to cause major environmental damage, interfering with marine and coastal biology and influencing human livelihoods for decades after a spill occurs.

In response to the Exxon Valdez spill, the United States Congress passed the 1990 Oil Pollution Act to prevent further oil spills from occurring in the United States. To improve prevention of future oil spills after Exxon Valdez, numerous models for analyzing oil spill risk were developed. In particular, during the Prince William Sound (PWS) Risk Assessment a system simulation of the PWS Maritime Transportation System (MTS) integrated shipping fleet data, traffic rules and operating procedures with accident frequency and consequence models (see, e.g., Merrick et al., 2002). Although the trend in both frequency and volume of spills has gone down significantly over the decades, the environmental risk of oil spills remains significant and severe because of both the immensity of worldwide maritime transportation, the large amounts of oil transported by a typical tanker, and the increased likelihood of vessels interacting with each other due to traffic growth in harbors and waterways. From 1995 to 2004, over three quarters of spills greater than 7 tons were caused by collisions and groundings (Huijer, 2005).

A widely accepted analysis model used in determining the oil outflow volume in tanker accidents was drafted by the International Maritime Organization in (1995). The purpose of the IMO (1995) model is to measure outflow performance of a particular tanker design against a reference double-hull design. It was constructed using approximately 100 historical collision and grounding scenarios from the period 1980-1990 to establish three probability density functions (PDFs) for the longitudinal, transversal and penetration damage extents in a collision or grounding scenario. Unfortunately, the IMO (1995) model suffers from a number of fundamental limitations. For example, some of the objections raised by Brown (1996) and van der Laan (1997) are : (1) the model uses a single set of damage extent PDFs from limited single-hull data; realistically, however, this data should only be used to model single-hull accidents, (2) damage extents are treated as independent random variables when they are truly dependent variables, and should be described using a joint PDF, and (3) the model does not have the ability to take the specifics of an accident scenario such as vessel speeds, displacement and interaction angle into account.

In 2001, the Marine Board of the National Academy of Science (NAS) published the SR259 report (NRC, 2001). It too noted that the IMO (1995) model was insufficient for double-hull tanker design evaluation. The SR259 report goes on to evaluate single-hull and double-hull tanker designs for both collisions and groundings using an alternative methodology. The SR259 publication reports

on physical simulations of accident damage inflicted on a tanker using the simulation programs SIMCOL and DAMAGE. SIMCOL is a collision analysis program developed by Brown (2001) that improves on the earlier work of Minorsky (1959). It was used to perform the collision analyses for the SR259 report. A joint Massachusetts Institute of Technology (MIT)-Industry Project on Tanker Safety (1992–2000) carried out research on plastic deformation of a ship's structure given a variety of impact scenario's (see, Simonsen and Wierzbicki 1996, 1997 and Simonsen 1998). Computation models from this research were implemented in the software DAMAGE and this software was used by Tikka (2001) to perform the grounding analyses for the SR259 report. The SR259 report describes the analysis results of 10,000 collision and grounding scenarios that were randomly generated and processed through these physical simulation programs using two single-hull and two double-hull tanker designs. This resulted in a data set of 40,000 collisions and 40,000 groundings, albeit simulated, describing jointly input (i.e. ship speed, displacement, collision angle) and output variables (i.e. damage length, outflow volume). Their goal of having these large data sets was to compare typical outflow performance between single-hull and double-hull tankers across a large variety of accident scenarios which were not related to a specific geographic context.

The physical simulation programs SIMCOL resp. DAMAGE described above are computationally extensive by themselves and therefore do not allow for direct consequence model integration with an also computationally intensive MTS simulation approach within a geographic context, similar to, e.g., the PWS Risk Assessment (Merrick et al., 2002). However, by carefully studying the relationships between input and output parameters of the large simulated data sets described in the SR259 report, one can "empirically" develop a model that (1) determines accident oil outflow based on statistical data analysis techniques rather can computationally intensive physical simulations and (2) adheres to the same physical principles imbedded in the models used in the SR259 report. More importantly, an oil outflow model that explicitly describes the "albeit" statistical relationships between the input parameters and the output parameters can be integrated with an MTS simulation approach. Indeed, the context of the oil outflow model developed herein was a vessel oil transportation risk assessment study from 2006-2008 in the Puget Sound and surrounding waters. It was conducted by a consortium of universities: The George Washington University, Virginia Commonwealth University, and Rensselear Polytechnic Institute. The oil transportation routes in question traverse the San Juan Islands and the Straits of Juan de Fuca. The San Juan Islands area is considered an environmentally pristine area and serves as a habitat for an Orca whale family. Moreover, the San Juan Islands and the Strait of Juan de Fuca are fishing grounds for both commercial and tribal salmon, crab and shrimp fisheries. This particular study builds on the MTS risk simulation approach developed for the Prince William Sound Risk Assessment (see, e.g., Merrick et al., 2002).

In Section 2, we shall briefly describe the input and output data from the SR259 report (NRC, 2001) that serve as data for the construction of our oil outflow models. In Section 3, we shall describe our methodology towards the oil outflow model for collisions in detail. Since the grounding oil outflow model is similar in construct, we shall only highlight some of the differences between the two in Section 4. In Section 5, we shall demonstrate a direct application of the collision and grounding oil outflow models by integrating them as the final analysis layer within an MTS risk simulation example. In this example, we shall evaluate the difference in performance of single-hull and double-hull tankers design against the back drop of a one year MTS simulation of oil transportation routes and surrounding traffic that traverse the San Juan Islands and the Straits of Juan de Fuca in Washington State.

2. A description of input and output data available in the SR259 Report

The SR259 report (NRC, 2001) describes 10,000 sets of input variables for both collisions and groundings that were subsequently fed into a physical simulation model. These simulations were performed on four different tanker designs, resulting in a total of 80,000 accident scenarios; each jointly describing a set of input and output variables. The tanker designs considered are a 40,000 DWT single-hull (SH40) and double-hull (DH40) tanker and a 150,000 DWT single-hull (SH150) and double-hull (DH150) tanker. In this section, the ship designs, the input variables, and resulting output variables are described in more detail.

An oil tanker is mainly characterized by its cargo area, which consists of one or more tanks or compartments. The cargo capacity is typically measured in deadweight tonnage (DWT) representing cargo mass. A vessel's displacement equals the water mass that the ship displaces. Among tankers, single-hull and double-hull designs are most commonly used. As the name implies, in a single-hull design only one wall separates the cargo compartments from the surrounding water; in a double-hull design, these compartments are protected by double walls that also serve as ballast tanks. The full schematic designs of the SH40, SH150, DH40 and DH150 tankers can be found in the SR259 report. Figure 1 is an adaptation of one of these schematics for the SH150 and DH150 designs. Table 1 provides the overall dimensions and tonnages for the SH40, SH150, DH40 and DH150 tanker designs.

In a collision, an oil tanker is struck by a ship. The collision transforms translational motion mainly into rotational motion, elastic deformation and plastic deformation. It is assumed in the SR259 report that the striking ship does not experience any damage. When a collision is severe enough, the hull of the oil tanker is penetrated and ruptured, resulting in a damaged area. If the damaged area overlaps with a compartment, all contents from this compartment are assumed spilled.

4
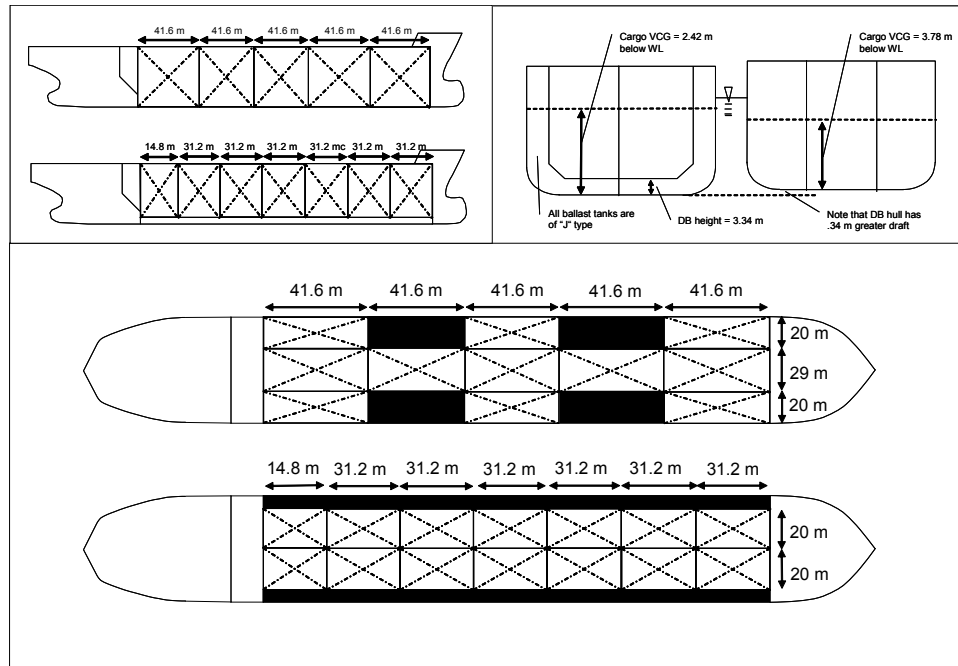
Figure 1. Single-hull and double-hull 150.000 DWT tanker designs adapted from SR259 report.

Table 1. Overall dimensions and tonnages of SH40, SH150, DH40 and DH150 tanker designs in SR259 report.

Name	Hull type	Length (Meters)	Beam (Meters)	Draft (Meters)	Deadweight Tonnage (Metric Tons)	Displacement (Metric Tons)
SH40	Single	201.17	27.40	10.60	40,000	47,547
SH150	Single	266.30	50.00	16.76	150,000	175,882
DH40	Double	190.50	29.26	10.58	40,000	47,448
DH150	Double	261.00	50.00	16.76	150,000	175,759

In a grounding, a tanker collides at the bottom with an obstacle, a cone shaped rocky pinnacle with a rounded tip. The rock is assumed fixed and strong enough never to suffer any damage. The input variables for the 40,000 collisions scenarios and the 40,000 grounding scenarios in the SR259 report are listed in Table 2.

Values for the following output variables are generated in the SR259 Report per tanker design using the 10, 000 collision simulation input scenarios:

$$\text{Damage length } y_l \text{ (meters),} \tag{1}$$
$$\text{Maximum penetration } y_t \text{ (meters) and}$$
$$\text{oil outflow } z \text{ (cubic meters).}$$

Damage length y_l is the extent of the damaged area in the struck ship's longitudinal direction.

5

Maximum penetration y_t is the maximum extent of the damage in a transversal direction. Oil outflow z is the total sum of volumes of damaged compartments, i.e. compartments that coincide with the damaged area. It must be noted that, whenever outflow occurs, y_l and y_t are strictly positive; however, the reverse is not always the case. Therefore, collision scenarios with damage but no outflow do occur, for example in the case of plastic deformation without hull breach, or the rupture of ballast tanks. This is more prevalent in double-hull tankers, where all oil compartments are separated from the outer hull by ballast tanks. Specifically, the percentages of zero oil outflow for the different tankers designs SH40, SH150, DH40 and DH150 were respectively $\approx 60\%$, 68%, 86% and 90%. Since the 10,000 collisions scenarios in terms of the striking vessel are the same for each tanker design, one immediately observes an initial benefit of the double-hull design over the single-hull designs.

Table 2. Input variables for 80,000 simulation scenarios in the SR259 report;
A: Collision input variables B: Grounding input variables.

A	Input Variable	Symbol	Unit
	Striking ship velocity	v_1	knots
	Struck ship velocity	v_2	knots
	Collision angle	Φ	degrees
	Displacement of striking vessel	m_1	1000 metric tons
	Collision location, relative from the stern	l	-
	Striking ship type	t	-
B	**Input Variable**	**Symbol**	**Unit**
	Striking ship velocity	v	knots
	Obstruction depth from mean low water	o_d	meters
	Obstruction apex angle	o_a	degrees
	Obstruction tip radius	o_r	meters
	Rock eccentricity	c	-
	Tidal varation from mean low water	τ	meters
	Inert tank pressure	p	mm water gauge
	Capture in ballast tank	b	% of tank volume
	Minimum outflow	ν	% of ruptured tank volume

Values for output variables similar to those described by (1) are generated for $40,000$ simulated grounding scenarios in the SR259 report. For example, each grounding scenario provides: (a) the begin and end locations of damage over the length of the vessel (from which y_l follows); (b) the damage over the width of the vessel (and hence we shall also use here the notation y_t in (1) for this

transversal damage); (c) a damage elevation y_v (which can be interpreted as a vertical damage penetration) and (d) the oil outflow z.

### 3. Construction of a collision oil outflow model

The joint availability of input and output collision data as discussed in Section 2 is used to construct a model that explicitly calculates outflow volume given a collision scenario. The essence of this model is to establish a relation between known input (velocity, collision angle, etc.) and output (longitudinal and transversal damage extents) data points so that given a particular tanker design, outflow can be calculated in a computationally efficient manner for any given collision scenario. For that reason, just searching through a set of 40,000 data points to find a match is not practical. Moreover, if the scenario in question is not amongst the 40,000 that were simulated, one needs to make some projections between these data points. A subsequent issue is that directly linking a set of input variables to outflow volume is not desired. Only a finite number of different possible outflow values are observed in the simulated output data of the SR259 report. This is a direct consequence of (1) utilizing the specified tanker designs SH40, SH150, DH40 and DH150 and (2) the assumption that all oil in a damaged compartment is lost. However, since the SR259 data contains the size of a damaged area in addition to the ship's design, it is possible to adopt the following stepwise modeling approach:

Step 1. Calculate the damage extents to the struck ship given arbitrary scenario input variables;
Step 2. Determine the probability of rupture given evaluated damage extents;
Step 3. Calculate the oil spill volume given rupture, damage extent and tanker design.

Since data is available for four different tanker design, the above stepwise modeling procedure will have to be executed four times, each estimating the accidental outflow volume based on the SH40, SH150, DH40 and DH150 designs. Finally, combining simulation data sets SH40 and SH150 (DH40 and DH150) results in an interpolation model for single-hull (double-hull) tankers between the SH40 and SH150 (DH40 and DH150) tanker sizes. Thus, in total six models were developed: four based on a particular design and two for interpolation purposes.

Figure 2 provides a schematic overview of the overall model construction and the analysis techniques used in the three sequential steps above for each of these six cases. Specifically, collision scenario variables serve as input to the "Step 1: Damage calculation" of the oil outflow model. The coefficients for this calculation are obtained through a polynomial regression analysis that uses the simulation input data outlined from the SR259 report outline in Table 2A and simulation output data described by (1) from 10,000 collision scenarios. The results from the "Step 1 Damage Calculation" serve as input to the "Step 2: Probability of rupture calculation" of the oil outflow

7

model. The coefficients for the latter calculation are obtained using a binary logistic regression analysis that uses the simulation damage and oil outflow output data from the SR259 report. Finally, the outputs of Steps 1 and 2 in the oil outflow calculation model, combined with input collision scenario variables (specifically, impact location and interaction angle), serve as input to "Step 3: Outflow volume". It is important to note that only the analysis in Step 3 requires the specification of a particular tanker design, along the lines of Figure 1, together with tank compartment capacities. The coefficients for Step 3 follow from a damage location analysis that uses physical simulation input, damage and oil outflow data from the SR259 report.
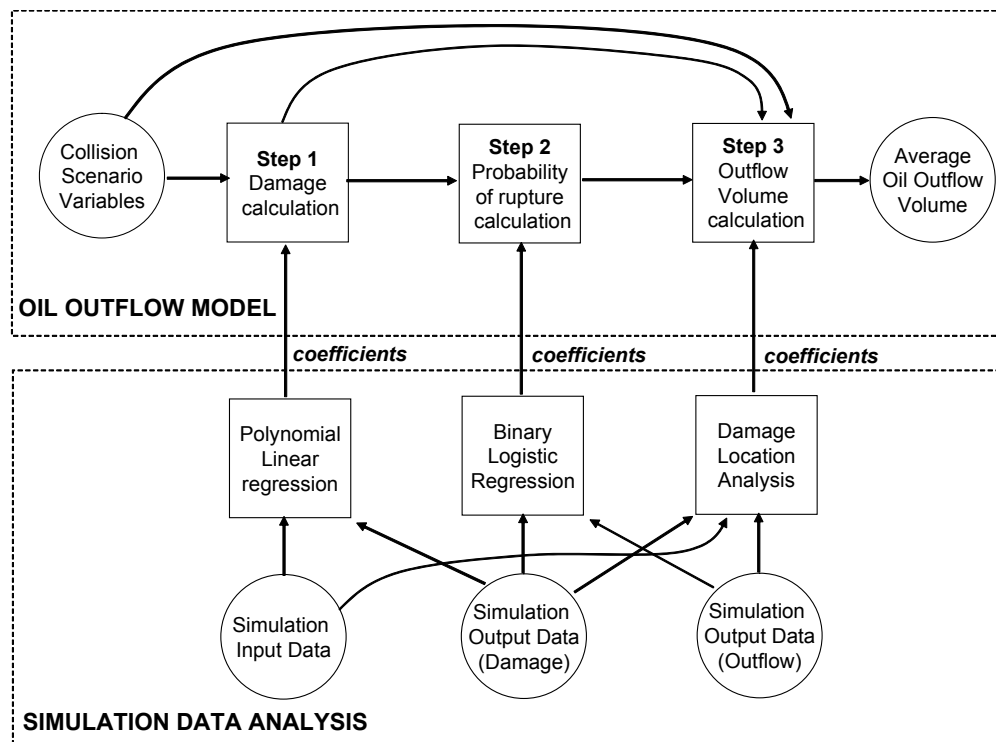
Figure 2. Collision modeling overview

The subsections below discuss the analytical methods used in the simulation data analysis box of Figure 2 to estimate the coefficients required for the oil outflow model. One of the challenges in the data analysis below is that traditional statistical model selection procedures fail when dealing with extremely large data sets (which we have). Schmeisser (1999) states:

> "*The fallacy of the goodness-of-fit test is made obvious when a large real-world data set is fitted to many classical distributions and all are rejected; all are rejected because the large sample size yields large power and the error in the model is indeed statistically significant.*"   (2)

8

Hence, rather than relying on statistical concepts such as p-values for model selection, we shall utilize well known goodness-of-fit heuristics such as R^2 values as well as visual goodness-of-fit tools such as probability and QQ plots for model selection. These are universally applicable regardless of the size of a data set.

3.1. Data modeling and analysis for Step 1 damage calculation coefficients

Intuitively, when traveling at the same speeds, a heavy ship will release more kinetic energy in a collision than a light one and a fast-moving ship will release more kinetic energy than a slow-moving one with the same mass as the former. Hence, damage extent in a collision is related to kinetic energy. In fact, a relationship between dissipated energy in a collision and damage volume has been established empirically by Minorsky (1959). Minorsky's model also served as a foundation for the enhanced physical simulation analysis used in the SR259 report and implemented in the SIMCOL software. SIMCOL was developed and enhanced by A. Brown over a number of years and its progress over time is described in Crake (1995), Brown and Amrozowicz (1996), Rawson et al. (1998), Chen (2000) and Brown (2001).

In the spirit of Minorsky's approach, the variables (v_1, v_2, m_1, ϕ) in Table 2A are used together with the tanker displacement m_2, to evaluate a perpendicular kinetic (k) energy predictor variable, denoted $e_{k,p}$, and tangential one, denoted $e_{k,t}$. A definition of $e_{k,p}$ and $e_{k,t}$, needs to take the relative direction of motion of the two vessels into account. When two colliding ships travel in a similar direction, less energy is released on a collision than when going in an opposite direction. Secondly, if the interaction angle ϕ is very oblique, the striking ship will likely cause less damage than when it strikes perpendicular to the struck ship's longitudinal axis. These concepts are further exemplified in Figure 3.

Let $\underline{v}_2 = \begin{pmatrix} v_2 \\ 0 \end{pmatrix}$ be the speed vector of the tanker, $\underline{v}_1$ be the speed vector of the striking vessel such that $|\underline{v}_1| = v_1$ and the interaction angle ϕ be defined as in Figure 3. Denoting the resulting speed vector $\underline{v}_r$, we have

$$\underline{v}_r = \underline{v}_2 - \underline{v}_1 = \begin{pmatrix} v_2 + v_1\cos\phi \\ v_1\sin\phi \end{pmatrix} = \begin{pmatrix} v_t \\ v_p \end{pmatrix} \tag{3}$$

where v_t is the resulting speed component tangential to the tanker and v_p is the resulting speed component perpendicular to the tanker. The following definitions of perpendicular and tangential kinetic energy then take the relative direction and speed of the striking vessel into account:

$$e_{k,t} = \frac{1}{2}m_{tot}v_t^2, \; e_{k,p} = \frac{1}{2}m_{tot}v_p^2. \tag{4}$$

where $m_{tot} = m_1 + m_2$, or the sum of displacements of both vessels. From (3) and (4) it can be derived that

$$e = \frac{1}{2} m_{tot} ||\underline{v}_r||^2 = e_{k,t} + e_{k,p}. \tag{5}$$

In other words, tangential kinetic energy $e_{k,t}$ and perpendicular kinetic energy $e_{k,p}$ as defined by (4) decompose the "collision kinetic energy" e defined by (5).
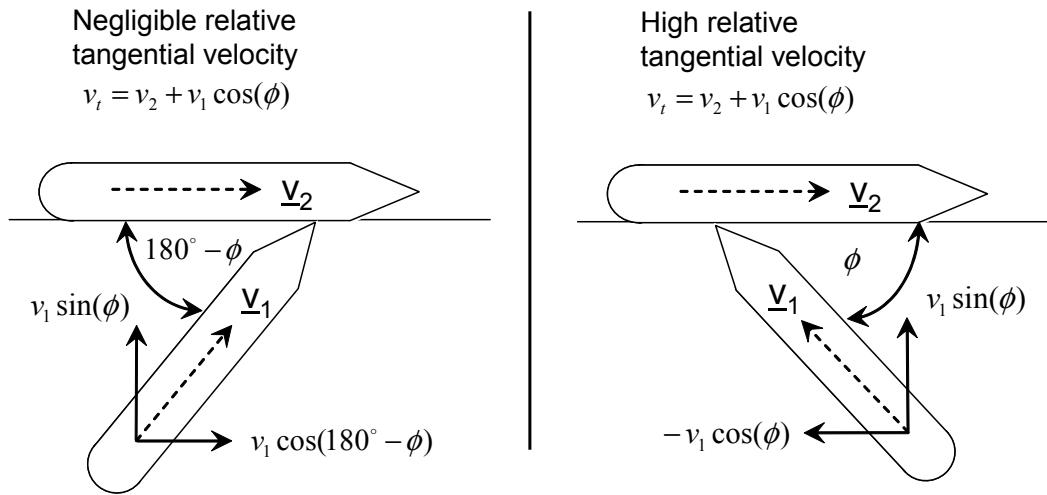
Figure 3. Definition of interaction angle ϕ.
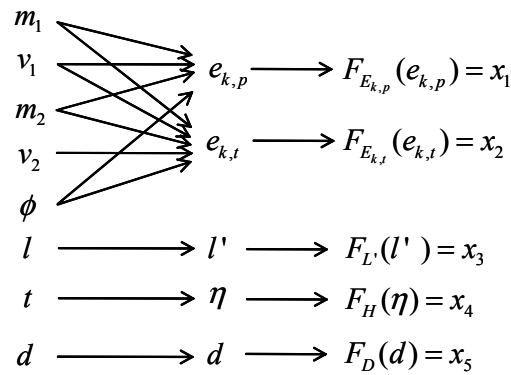**Vessel 1 is the striking vessel and Vessel 2 is the tanker.**

Perpendicular bulkheads are upright partitions over the length of a ship dividing it into compartments and serve to add structural rigidity, among other things. The most forward one along the bottom plane of the ship is referred to as the Forward Perpendicular (FP). Analagously, the most rear one towards the stern of the vessel is referred to as the Aft Perpendicular (AP). The input variable l in Table 2A specifies the relative distance of the collision location from the AP bulkhead of the tanker. The value $l = 0$ in the SR259 report means the collision takes place at the AP, whereas $l = 1$ represents a collision at the FP bulkhead. To capture a rotational effect in our analysis we transform l to

$$l' = |l - \frac{1}{2}|, \tag{6}$$

which views the midpoint of a tanker as the origin or rotation axis. The striking ship type t listed in Table 2A provides information about its half bow angle η. Finally, an indicator variable d is used in a "combined" analysis by merging the data points for the smaller tanker designs with the larger ones

10

for interpolation purposes. Figure 4 summarizes the specification of predictor variables (or independent variables) from the input variables listed in Table 2A for a polynomial regression (see, e.g., Draper and Smith (1998)).

Natural logarithms of y_l and y_t were selected as dependent variables to achieve residual homoscedasticity, i.e. a constant variance behavior of residuals. Due to large observed differences in absolute values of $e_{k,p}$, $e_{k,t}$ and those of l', η and d, all predictor variables $e_{k,p}$, $e_{k,t}$, l', η and d are first normalized on a $[0, 1]$ scale using their observed distributions within the sample set of $10,000$ collisions available for each tanker design. This has the benefit that (1) regression coefficients can be compared pairwise, (2) the dimension of regression coefficients equals that of the dependent variable (since each independent variable is dimensionless) and (3) the estimated coefficients are not affected by the distributions chosen to generate the collision scenarios in the SR259 report.

$$
\begin{array}{c}
m_1 \\
v_1 \\
m_2 \\
v_2 \\
\phi
\end{array}
\quad
\begin{array}{l}
e_{k,p} \longrightarrow F_{E_{k,p}}(e_{k,p}) = x_1 \\
e_{k,t} \longrightarrow F_{E_{k,t}}(e_{k,t}) = x_2
\end{array}
$$

$$
l \longrightarrow l' \longrightarrow F_{L'}(l') = x_3
$$
$$
t \longrightarrow \eta \longrightarrow F_H(\eta) = x_4
$$
$$
d \longrightarrow d \longrightarrow F_D(d) = x_5
$$

Figure 4. Definition of interaction angle ϕ.
Vessel 1 is the striking vessel and Vessel 2 is the tanker.

Distributions had to be fitted for the derived data sets obtained for $e_{k,p}$ and $e_{k,t}$. A goodness-of-fit analysis resulted in selecting Weibull distributions to represent them. Figure 5A plots both the empirical and a fitted Weibull distributions for the $e_{k,p}$ values of the $10,000$ collision scenarios of the SH40 tanker design case. Figure 5B plots the Weibull probability plot of this fit. Figure 5B supports a good-fit conclusion of the Weibull model despite the small p-value observed in Figure 5B due to dealing with an extremely large data set (Recall (2)). Table 3 provides the parameters (evaluated using a least squares approach) of the fitted Weibull distributions for the scale transformations $F_{E_{k,p}}(\cdot)$ and $F_{E_{k,t}}(\cdot)$ in Figure 4. Generating distributions for l and t in Figure 4 were specified in the SR259 report and allow for a direct transformation to generating distributions of l' and η as indicated in Figure 4. Further details are provided in van de Wiel (2008).

Figure 6 exemplifies two polynomial regression profiles comparing the single-hull and double-hull combined cases. Figure 6A plots transversal damage extent y_t as a function of normalized

perpendicular kinetic energy $e_{k,p}$ defined by (4). Figure 6B plots transversal damage extent y_t as a function of normalized tangential kinetic energy $e_{k,t}$ also defined by (4). Other independent variables were fixed at their center points in plotting Figure 6. The y-axes in Figure 6 are measured in meters. We further observe from Figure 6 that the double-hull tanker design outperforms the single-hull tanker design.
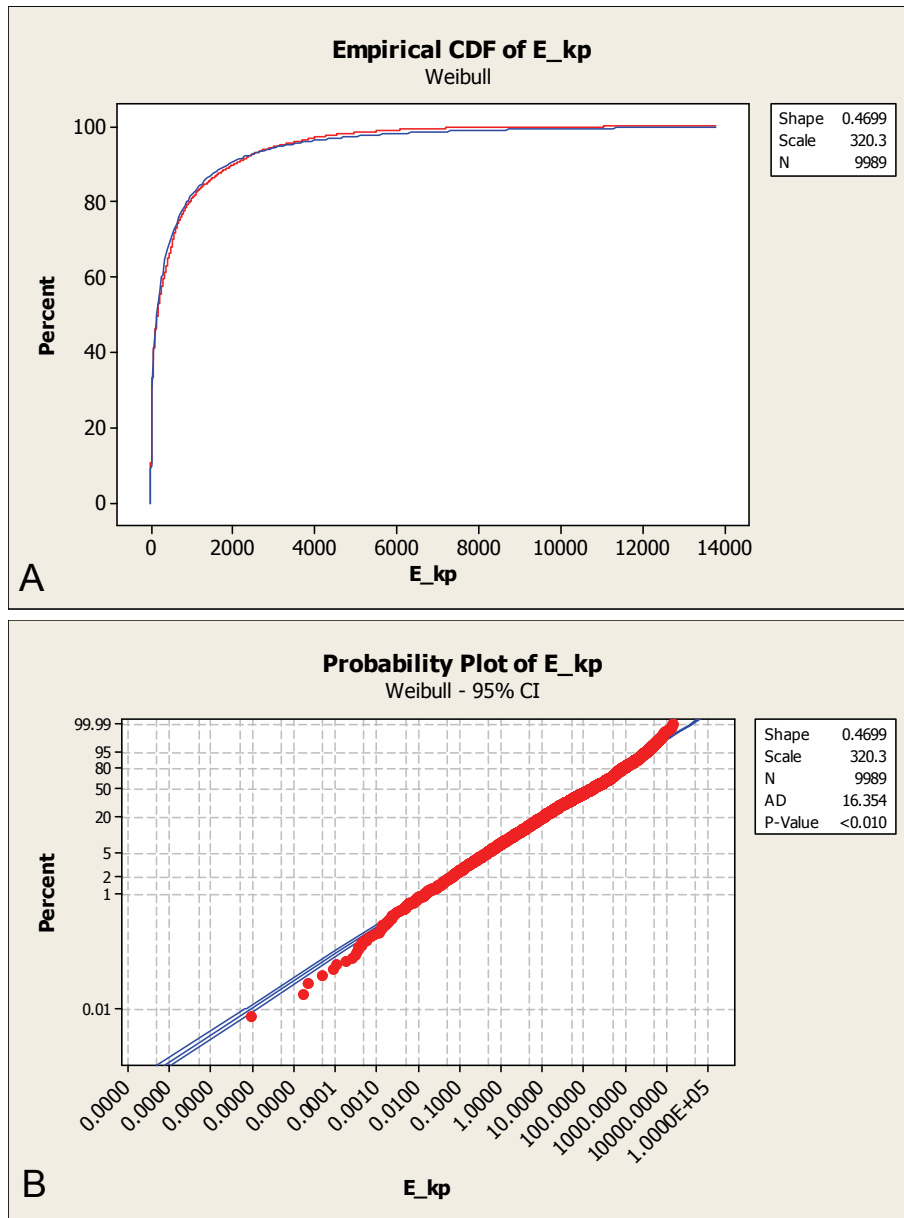

Figure 5. SH40 model selection procedure for $F_{E_{k,p}}(\cdot)$ using probability plots:
A: Empirical and fitted Weibull CDF of $e_{k,p}$ data; B: Probability plot of Weibull fit.
Table 3. Parameters of fitted Weibull distributions for $E_{k,p}$ and $E_{k,t}$ in Table 3.

		SH40	SH150	SHCOM	DH40	DH150	DHCOM
$E_{k,p}$	α	0.4699	0.4724	0.4515	0.4699	0.4724	0.4514
	β	320.3	1010	590	319.8	1010	589.4
$E_{k,t}$	α	0.4546	0.4567	0.4379	0.4546	0.4567	0.4378
	β	385.7	1217	709.9	385.1	1217	709.1

Table 4 provides the estimated coefficients of a polynomial regression analysis for the longitudinal damage extent $\ln(y_l)$. In Table 4, the row with β_0 contains the intercept values and $\beta_{i,j}$ are the regression coefficients of $(x_j)^i$, where $x_j, j = 1, \ldots, 5$ are described in Figure 4. Observe from Table 4 that R^2 values are about 70% for all polynomial regressions, which can be considered quite high. To attain these R^2-values, first a stepwise regression was performed on all variables $(x_j)^i, i, j = 1, \ldots, 5$ to select a candidate set of independent variables. Next, a best subset regression was performed on this set of candidate independent variables. Mallows C_p values (see, e.g. Bookrags, 2009) provide an indication of "overfitting" by a subset of variables and were used to ultimately arrive at the subset of variables indicated in Table 4. An analogous data analysis was performed for log transversal damage extents $\ln(y_t)$. Coefficients are available in van de Wiel (2008) or from the authors upon request.

3.2. Data modeling and analysis for Step 2 probability of rupture coefficients

Recall from (1) that z expresses the outflow volume in a collision scenario. Introducing the binary variable z' where

$$z' = 1_{[0,\infty)}(0) = \begin{cases} 1 & z > 0 \\ 0 & z = 0 \end{cases} \tag{7}$$

a binary logistic regression analysis (see, e.g., Homser and Lemeshow, 2002) can be performed with z' as the dependent variables and $\ln(y_l)$ and $\ln(y_t)$ as the independent variables. While Step 1 in Figure 2 yields values for $\ln(y_l)$ and $\ln(y_t)$, the binary logistic regression is conducted using the natural logarithms of damage length y_l and y_t provided for 10,000 collision scenarios per tanker design in the SR259 report. This removes the potential of propagating an estimation error in the evaluation of $\ln(y_l)$ and $\ln(y_t)$ in Step 1 of Figure 2 further into the evaluation of the coefficient parameters for Step 2 of the oil outflow calculation model. The regression model is expressed as follows:

$$E[Z'] = \pi[\ln(y_l), \ln(y_t)|\underline{\beta}] = \frac{exp[\beta_0 + \beta_l\ln(y_l) + \beta_t\ln(y_t)]}{1 + exp[\beta_0 + \beta_l\ln(y_l) + \beta_t\ln(y_t)]} \tag{8}$$

Table 4. Polynomial regression coefficients of order 5 for the natural logarithm of longitudinal damage $\ln(y_l)$ using the predictor variables outlined in Figure 4.

	SH40	SH150	SHCOM	DH40	DH150	DHCOM
Number of data points	7467	7473	14940	7454	7466	14920
R^2-value	70.9%	68.1%	68.9%	71.5%	69.9%	70.6%
Mallows C_p-value	19.0	19.8	13.1	14.2	24.0	16.0
Coefficients	**SH40**	**SH150**	**SHCOM**	**DH40**	**DH150**	**DHCOM**
β_0	-2.914	-2.661	-2.982	-2.931	-2.786	-2.632
$\beta_{1,1}$	3.078	-1.215	2.246	2.128	2.047	-0.117
$\beta_{2,1}$	5.550	5.303	5.231	6.180	4.692	4.670
$\beta_{3,1}$	0.031	-2.493	-3.369	0.708	-3.224	-1.973
$\beta_{4,1}$	0.546	1.613	1.188	0.655	1.429	1.155
$\beta_{5,1}$	-	-	0.223	-	-	0.052
$\beta_{1,2}$	-	10.181	0.687	0.598	-	5.792
$\beta_{2,2}$	-	-	-	-5.563	-	-
$\beta_{3,2}$	-	20.261	25.010	-	24.187	16.819
$\beta_{4,2}$	-	-0.931	-0.560	-	-0.784	-0.566
$\beta_{5,2}$	-	-	-	-	-	-
$\beta_{1,3}$	-	-8.145	-	-	-	-
$\beta_{2,3}$	-11.982	-6.405	-6.750	-	-5.410	-5.756
$\beta_{3,3}$	-	-68.750	-75.742	-13.309	-69.908	-53.668
$\beta_{4,3}$	-	-	-	-0.158	-	-
$\beta_{5,3}$	-	-	-	-	-	-
$\beta_{1,4}$	-2.924	-	-	-	-	-10.900
$\beta_{2,4}$	9.403	-	-	-	-	-
$\beta_{3,4}$	-	94.810	96.400	27.442	85.081	69.372
$\beta_{4,4}$	-	-	-	-	-	-
$\beta_{5,4}$	-	-	-	-	-	-
$\beta_{1,5}$	2.823	2.008	-	-	0.542	7.798
$\beta_{2,5}$	-	4.134	4.529	2.291	3.724	4.031
$\beta_{3,5}$	-0.480	-44.783	-43.224	-15.354	-36.872	-31.216
$\beta_{4,5}$	-	-	-	-	-	-
$\beta_{5,5}$	-	-	-	-	-	-
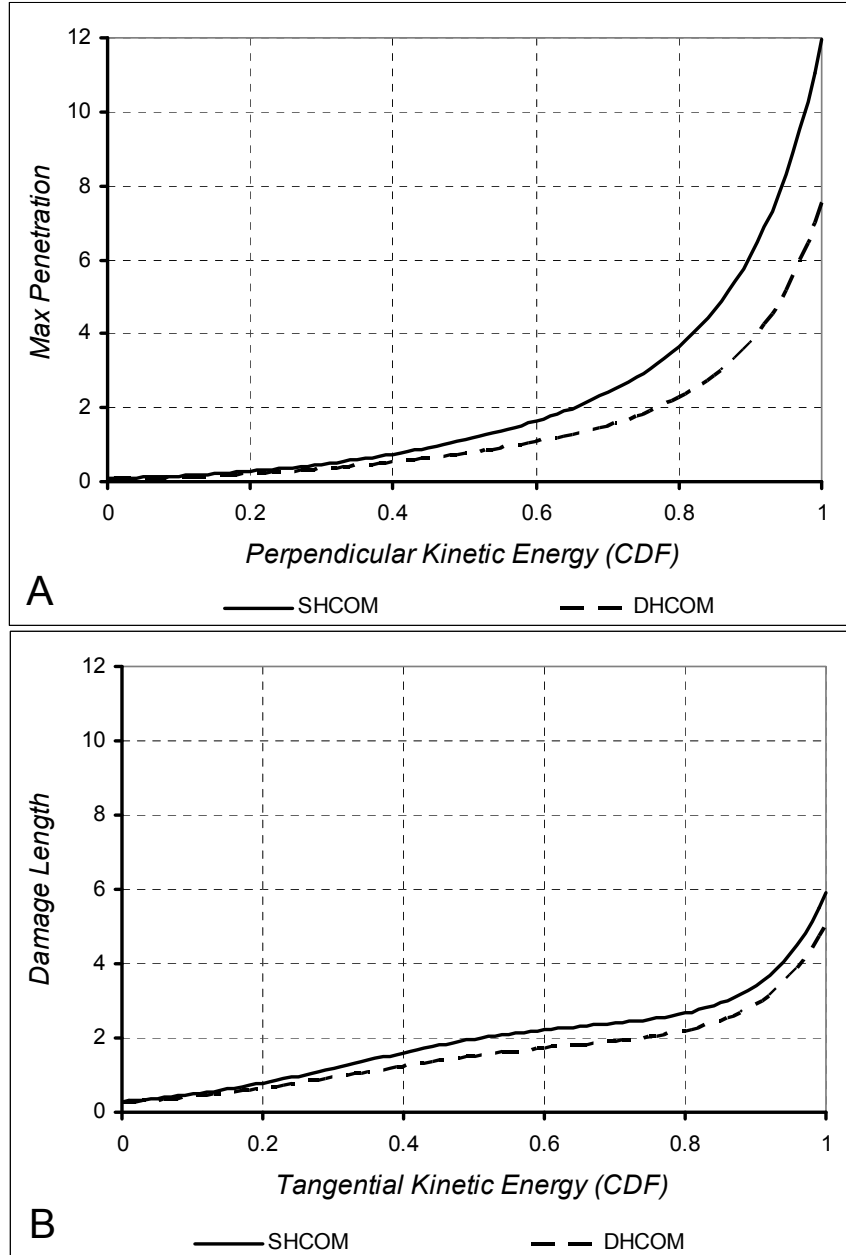
Figure 6. Polynomial regression profiles for single-hull and double-hull tankers
A: y_t as a function of $F_{E_{k,p}}(\,\cdot\,)$, B: y_l as a function of $F_{E_{k,t}}(\,\cdot\,)$

where observations (7) are interpreted as realizations of the random variable Z' in (8). The quantity $\pi[\ln(y_l), \ln(y_t)|\underline{\beta}]$ in (8) may be interpreted as the probability of oil compartment tank rupture as a function of log-longitudinal damage extent $\ln(y_l)$ and log-transversal damage extent $\ln(y_t)$. Parameters $\underline{\beta} = (\beta_0, \beta_l, \beta_t)$ are estimated via a maximum likelihood procedure (not to be confused with the polynomial regression coefficients in Table 4). Table 5 provides the resulting coefficients $\underline{\beta} = (\beta_0, \beta_l, \beta_t)$ for (8) for each of the tanker designs.

15

Table 5. Logistic regression coefficients for probability of rupture $\pi[\ln(y_l), \ln(y_t)|\underline{\beta}]$ as defined by (8) for each tanker design and the interpolation cases.

	SH40	SH150	SHCOM	DH40	DH150	DHCOM
No. Cases	7740	7430	14811	7423	7436	14788
Coefficients						
β_0	-0.229	-0.864	-0.511	-7.026	-10.823	-7.142
β_t	0.162	0.164	0.158	5.943	7.330	5.443
β_l	0.536	0.514	0.498	0.257	0.283	0.143

Unfortunately, traditional logistic regression goodness-of-fit tests suffer from the same deficiencies when dealing with extremely large data sets as previously indicated by Schmeisser (1999) (recall (2)). To evaluate visually if $\ln(y_l), \ln(y_t)$ have explanatory power in terms of the observations z', we generate two sets of residuals

$$r_{OUT,i} = z'_i - \pi[\ln(y_{l,i}), \ln(y_{t,i})|\widehat{\underline{\beta}}] \text{ and } r_{RND,i} = z'_{RND,i} - \pi[\ln(y_{l,i}), \ln(y_{t,i})|\widehat{\underline{\beta}}], \qquad (9)$$

where the index i represents a particular collision scenario from the SR259 report, z'_i are indicator values (7) describing whether oil outflow occurred in the SR259 collision analysis, and $z'_{RND,i}$ are randomly generated Bernoulli coin tosses with probability p where

$$p = \frac{\text{\# outflow events}}{\text{\# events}}. \qquad (10)$$

In the event that that independent variables $\ln(y_l), \ln(y_t)$ in (8) do <u>not</u> have explanatory power, one would expect a QQ plot of the empirical distributions of $r_{OUT,i}$ and $r_{RND,i}$ to be a straight line. Figure 8 shows this QQ plot for the SH150 tanker design. One visually observes from Figure 8 that this QQ plot is <u>not</u> a straight line, and thus an explanatory power of $\ln(y_l)$ and $\ln(y_t)$ via (8) in the observations z' defined by (7) may be concluded.

To further enhance our QQ plot analysis we evaluate the point biserial correlation coefficient r_{pb} between z'_i and $\pi[\ln(y_{l,i}), \ln(y_{t,i})|\widehat{\underline{\beta}}]$. The point biserial correlation r_{pb}

$$r_{pb} = \frac{M_1 - M_0}{s_n}\sqrt{\frac{n_1 n_0}{n}}, s_n^2 = \frac{1}{n-1}\sum_{i=1}^{n}(z_i' - \overline{z}')^2 \qquad (11)$$

determines correlation between a continuously measured variable ($\pi[\ln(y_{l,i}), \ln(y_{t,i})|\widehat{\underline{\beta}}]$ in our case) and a dichotomous variable (z_i' defined by (7)). The integers n_1 and n_0 are the number of occurrences of 1 and 0 in the z' data and M_1 and M_0 are the mean values of the continuously measured variable conditioned on the value of z' (either 1 or 0, respectively). The test-statistic
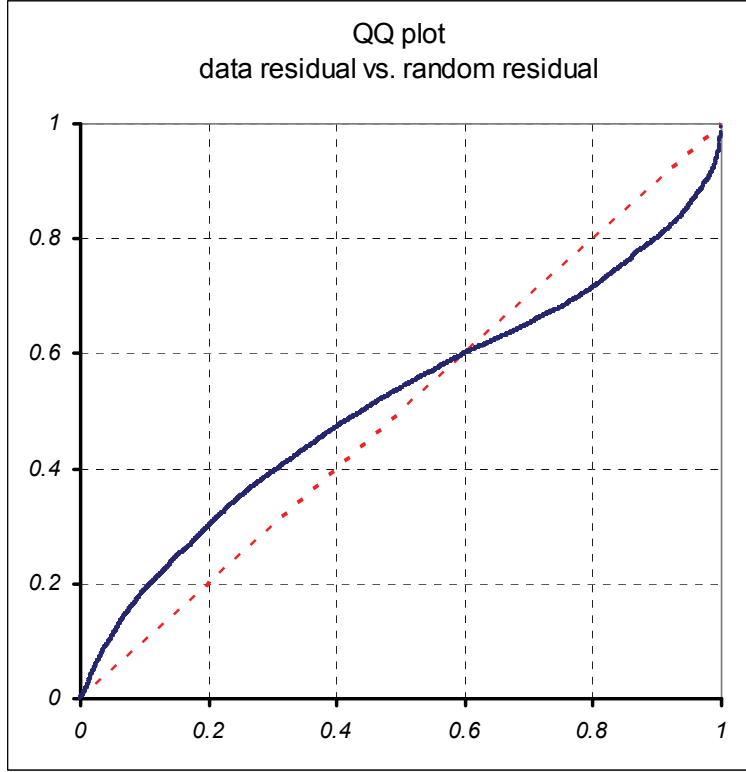
Figure 7. QQ Plot of empirical cdf's of $r_{OUT,i}$ **and** $r_{RND,i}$
defined by (9) for the SH40 tanker design.

$$t = r_{pb} \sqrt{\frac{n_1 + n_0 - 2}{1 - r_{pb}^2}} \tag{12}$$

is Student-t distributed with $n_1 + n_0 - 2$ degrees of freedom.

Table 6 provides the point biserial correlations per tanker design using between $\pi[\ln(y_{l,i}), \ln(y_{t,i}) | \widehat{\underline{\beta}}]$ and both the z_i' and $z_{RND,i}'$ data in (7) and (9). A zero correlation between $\pi[\ln(y_{l,i}), \ln(y_{t,i}) | \widehat{\underline{\beta}}]$ and z_i' would indicate no explanatory power of the logistic regression model (8) with the fitted parameters in Table 5. From the first row of p-values one observes that the null hypothesis of zero-correlation between $\pi[\ln(y_{l,i}), \ln(y_{t,i}) | \widehat{\underline{\beta}}])$ and z_i' is indeed rejected for all cases. As to be expected, and for comparison purposes, observe that one fails to reject the null-hypothesis of a zero correlation between the $z_{RND,i}'$ data in (9) and $\pi[\ln(y_{l,i}), \ln(y_{t,i}) | \widehat{\underline{\beta}}]$ (see the p-values in the fourth row of Table 6).

Figure 8 plots the behavior of the expected rupture probability $E[Z']$ of a tank compartment given by (8) as a function of log-transversal damage extent $\ln(y_t)$ and log-longitudinal damage extent $\ln(y_l)$ for the SH150 and DH150 tanker designs. Observe from Figure 8A strictly positive probabilities of rupture for the single-hull case for relatively low values of $\ln(y_t)$ and $\ln(y_l)$, whereas

17

in these same ranges a virtually zero oil tank rupture probability is observed for the double-hull design. Also observe from Figure 8A a larger effect of log-longitudinal damage $\ln(y_l)$ on tank compartment rupture for the SH150 than for the double-hull case DH150 in Figure 8B.

Table 6. Binary logistic regression point-biserial correlation tests.

	SH40	**SH150**	**SHCOM**	**DH40**	**DH150**	**DHCOM**
No. Cases	7740	7430	14811	7423	7436	14788
r_{bp} (data)	0.40	0.43	0.41	0.85	0.86	0.82
p-value (data)	0	0	0	0	0	0
r_{bp} (random)	-0.01	-0.02	-0.00	0.00	0.01	0.01
p-value (random)	0.50	0.17	0.78	0.80	0.36	0.14
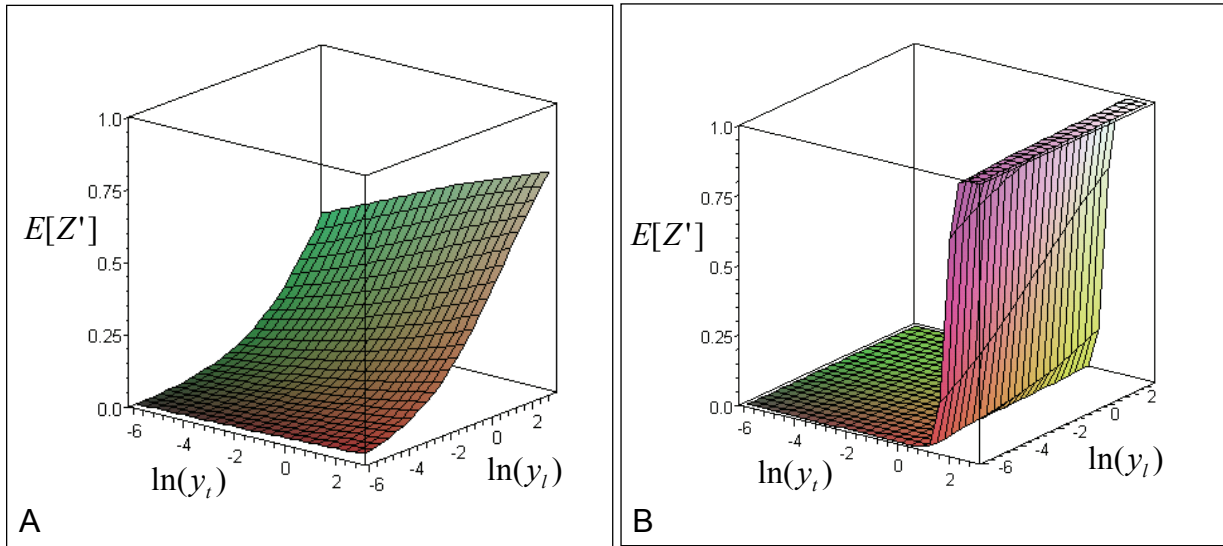
Figure 8. Expected probability of rupture $E[Z']$ given by (8) as function of $\ln(y_l), \ln(y_t)$, A: SH150 Tanker design; B: DH150 Tanker design.

3.3. Data modeling and analysis for Step 3 outflow volume coefficients

Based on damage length y_l, penetration depth y_t, and collision impact location l, Step 3 of the oil outflow model in Figure 2 involves calculating the oil outflow volume given that penetration has occurred. Our oil outflow model makes the worst case assumption that the damaged area is rectangular, its longitudinal and transversal dimensions being determined respectively by damage length (y_l) and penetration depth (y_t). Furthermore, each compartment that is covered by the damaged area is assumed to lose all its oil. For all four struck ship models, compartment configurations are available in the form of transverse and longitudinal bulkhead coordinates and compartment volumes (a schematic of one of these configurations is given below in Figure 9A).
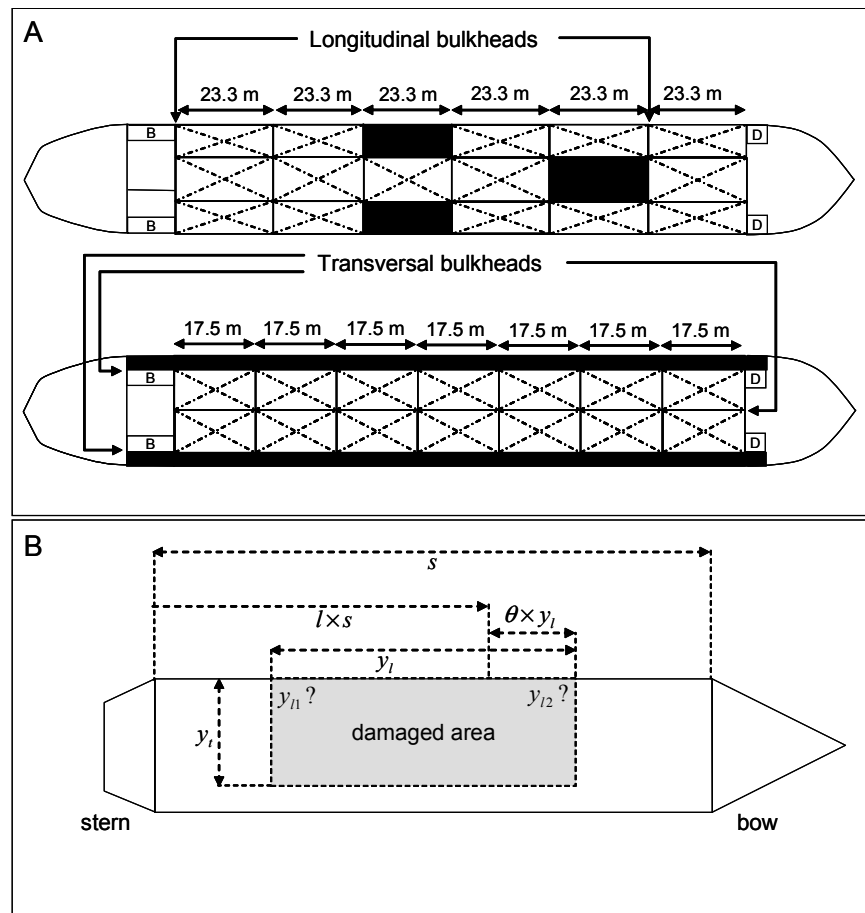
Figure 9. A: Bulkhead placement of SH40 and DH40 tanker designs;
B: Collision location (l) and damage length (y_l) are known,
start and end position (y_{l1}; y_{l2}) are unknown.

The collision of a container vessel (the Cosco Buscan) with a pillar of the San Francisco Bay Bridge in 2007 triggered the largest US oil spill in more than a decade (USCG, 2008). The oil loss in the accident above involved solely heavy bunker fuel. To also accommodate diesel fuel and bunker fuel oil outflow calculations, Figure 9A was augmented from its version in the SR259 report with approximate bunker fuel and diesel fuel compartment locations (indicated by B and D). While certainly more than two bunker fuel tanks and diesel fuel tanks on any given deep draft vessel are possible, the locations in Figure 9 for these vessel fuel tanks were modeled from a worst case analysis perspective. Bunker fuel compartments were located towards the stern (where the main engine is located) and diesel fuel compartments towards the bow. Note that from Figure 9 it follows that a double-hull tanker is provided the benefit of the double-hull for the diesel fuel and bunker fuel compartments as well.

In each accident scenario, the longitudinal position of the damaged area is determined by the relative collision location l. However, neither start nor end coordinates are provided in the output data of the SR259 report for collisions, only the damage length y_l. Therefore, we model start and end coordinates (y_{l1}, y_{l2}) by using ship length s, (see also Figure 9B) by setting:

$$\begin{cases} y_{l_1} = (1-\theta)y_l + (1-l)s \\ y_{l_2} = -\theta y_l + (1-l)s \end{cases} \tag{13}$$

where $\theta \in [0,1]$ is a function of the collision interaction angle ϕ (see Figure 3) and the tangential relative speed component v_t along the struck vessel, and (y_{l_1}, y_{l_2}) are measured from the FP perpendicular bulkhead. If $\phi = 90°$ and $v_t = 0$, we set $\theta = \frac{1}{2}$ and the collision location is in the middle of the longitudinal damage. If $\phi = 0°$, then all longitudinal damage is behind the collision location l as measured from the forward point and we set $\theta = 0$. If $\phi = 180°$ then all longitudinal damage is in front of the collision location and we set $\theta = 1$.

The following model is adopted for the evaluation of θ for intermediate values of the collison interaction angle ϕ and the tangential relative speed component v_t

$$\theta(\phi, v_t | m, n) = \begin{cases} 0, & \phi = 0, \\ \left[\frac{1}{2}\left(\frac{\phi}{90}\right)^n \right]^{exp(mv_t)}, & 0 < \phi \leq 90, \\ \left[1 - \frac{1}{2}\left(\frac{180-\phi}{90}\right)^n \right]^{exp(mv_t)}, & 90 \leq \phi < 180, \\ 1, & 1. \end{cases} \tag{14}$$

where parameters $m, n \geq 0$. The behavior of the model (14) is exemplified in Figure 10. Figure 10A, demonstrates that when $m = 0$ or $v_t = 0$ in (14), longitudinal damage extent is symmetrically distributed from the impact location l in case the interaction angle is perpendicular $(\phi = 90°)$ and is unevenly distributed with more damage in the direction of striking vessel for other values of ϕ. Figure 10B demonstrates the effect of the parameter n for a fixed interaction angle ϕ (while keeping m or v_t fixed at 0). In the case where the tangential relative speed component $v_t \neq 0$, it is clear that v_t may impact the distribution of longitudinal damage across the impact location l. Hence, the inclusion of the parameter $m \geq 0$ and v_t in the model (14) becomes necessary.

The parameters m and n are fitted based on the least squares approach using evaluated oil outflow given a certain value for m and n across $10,000$ collision scenarios for a particular tanker design and by comparing them to the evaluated oil outflows provided by the SR259 report. Table 7 provides the parameter estimates for m and n and the percentage of time that our model evaluates exactly the same oil outflow volume as the SR259 report, given impact location l, longitudinal damage y_l, transversal damage y_t, interaction angle ϕ and tangential residual velocity v_t. Observe

from the second row that about more than 95% of the collision scenarios the oil outflow volumes of both models coincide.
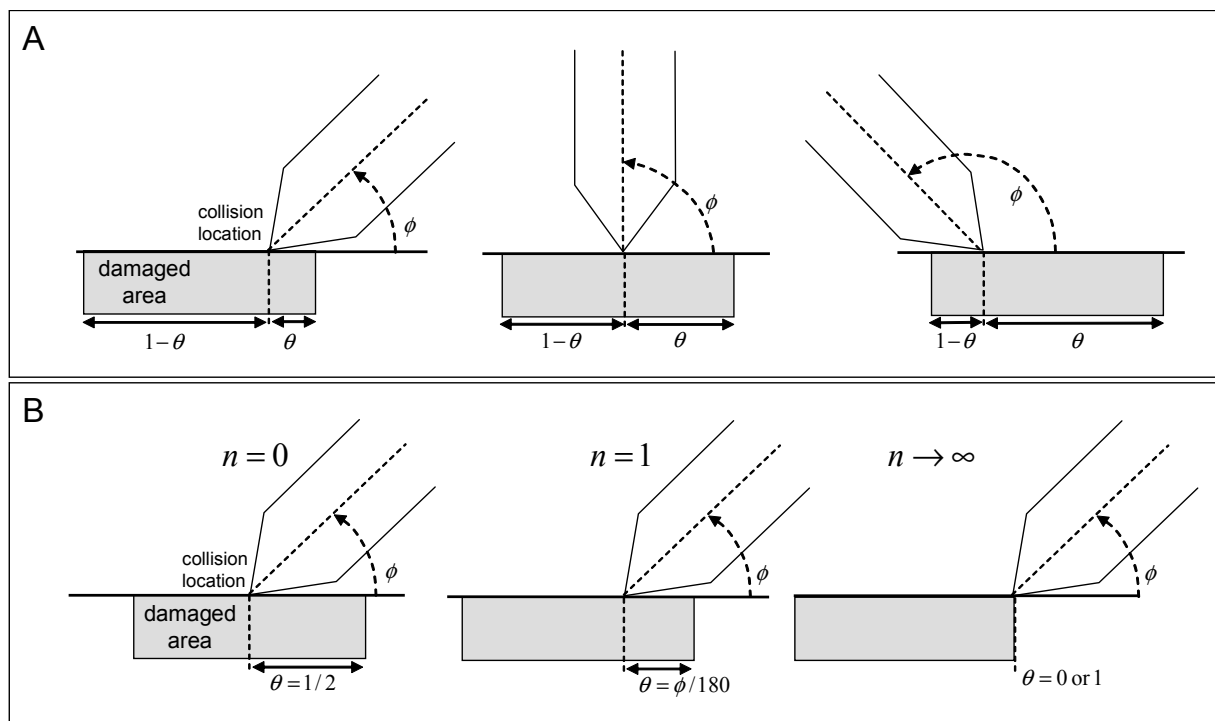

Figure 10. Behavior of model (14) to evaluate $(y_{l1}; y_{l2})$ given impact location l, interaction angle ϕ and relative tangential velocity v_t; A: $m = 0, n = 1$; B : $m = 0$

Table 7. Fitted parameter values of m and n in (14) by tanker design.

	SH40	SH150	SHCOM	DH40	DH150	DHCOM
No. Cases	4045	3183	7228	1404	1026	2430
% correct predictions	97.11%	97.86%	97.40%	94.87%	96.78%	95.60%
m	0.112	0.098	0.112	0.061	0.091	0.091
n	5.90	6.20	5.91	4.59	5.60	5.62

3.4. Example calculation

Tables 8 and 9 detail a sample calculation of a collision scenario of a $50,000$ metric ton vessel traveling at 12 knots at an interaction angle of 45 degrees, with a tanker (SH150 in Table 8 and DH150 in Table 9) traveling at 5 knots. The half bow angle of the striking vessel is 25 degrees. Since we are dealing with the larger tankers the indicator variable d is set to 1. The values in the column "predictor variables" in Tables 8 and 9 follow from expressions (4), (6) and the transformations

displayed in Figure 4. Since the dimensions and displacement of both the SH150 tanker and the DH150 tanker are very close, no difference is observed (at an accuracy of three decimals) in the second columns of Table 8 and 9 in terms of the transformed perpendicular and tangential kinetic energy. However, different values are observed in terms of the analysis results that follow from Step 1, 2 and 3 of the oil outflow model in Figure 2 using the resulting coefficients estimated as described in Sections 3.1, 3.2 and 3.3.

Table 8. Calculation results for example collision scenario with SH150 tanker.

Input Variables	Predictor Variables	STEP 1	STEP 2	STEP 3
$v_1 = 12$ knots	$F_{E_{k,p}}(e_{k,p}) = 0.962$	$y_l = 29.249$	$\pi = E[Z'] = 0.976$	$y_{l_1} = 79.89$
$m_1 = 50 \cdot 10^3$ mtons	$F_{E_{k,t}}(e_{k,t}) = 0.987$	$y_t = 9.863$		$y_{l_2} = 109.14$
$v_2 = 5$ knots				
$\phi = 45°$				
$l = 0.7$	$F_L(l') = 0.465$			
$\eta = 25°$	$F_H(\eta) = 1$			
$d = 1$	$F_D(d) = 1$			

Table 9. Calculation results for example collision scenario with DH150 tanker.

Input Variables	Predictor Variables	STEP 1	STEP 2	STEP 3
$v_1 = 12$ knots	$F_{E_{k,p}}(e_{k,p}) = 0.962$	$y_l = 21.854$	$\pi = E[Z'] = 0.822$	$y_{l_1} = 78.30$
$m_1 = 50 \cdot 10^3$ mtons	$F_{E_{k,t}}(e_{k,t}) = 0.987$	$y_t = 6.789$		$y_{l_2} = 100.15$
$v_2 = 5$ knots				
$\phi = 45°$				
$l = 0.7$	$F(l') = 0.465$			
$\eta = 25°$	$F_H(\eta) = 1$			
$d = 1$	$F_D(d) = 1$			

Now, for the SH150 tanker, the location of affected compartments have to be determined from y_{l_1}, y_{l_2} and y_t. From Figure 2 and the penetration depth $y_t = 9.863$ it follows that only outer compartments can be of the affected. From $y_{l_1} = 79.89$ and $y_{l_2} = 109.14$ and Figure 1 it follows that the longitudinal damage runs across the 3rd and 4th compartment as counted from the Aft Perpendicular (AP), the 4th one being a ballast tank containing no oil. Hence, the total capacity of oil for these two compartments equals the capacity of the 3rd compartment of $15,311m^3$. Combined with the probability of rupture 0.976 in Table 8 this yields an average oil outflow for the SH150 tanker of $15,311 \times 0.976 \approx 14,944m^3$ for the collision scenario in Table 8.

In the DH150 case, the depth penetration of $y_t = 6.789$ is deep enough to have the potential of rupturing the second wall (see also Figure 1.). From $y_{l_1} = 78.30$ and $y_{l_2} = 100.15$ and Figure 1 it follows that the longitudinal damage only runs across 4th compartment as counted from the AP. The double-hull compartment contains ballast and no oil. Hence, the total capacity of oil for these two compartments equals the capacity of the 4th compartment of $14,561m^3$. Combined with the

probability of rupture 0.822 in Table 9 this yields an average oil outflow for the DH150 tanker of $14561 \times 0.822 \approx 11{,}970m^3$ for the collision scenario in Table 8.

   This particular collision scenario demonstrates a significant benefit for the double-hull design in analysis Table 9 ($11{,}970m^3$) relative to the single-hull design analysis in Table 8 ($14{,}944m^3$), a reduction of approximately 20% in oil outflow. It is not larger in this scenario since the depth penetration y_t has the potential of rupturing the second wall of the DH150 design in Figure 1. A larger benefit would have occurred for those collision scenarios that do not have the potential to penetrate the second wall due to smaller values of transversal damage y_t. From this particular collision scenario one may also observe, however, a potential benefit of the single-hull SH150 tanker design compared to DH150 tanker. Indeed, given a large depth penetration y_t, the SH150 tanker has the advantage of sometimes being hit in a ballast compartment, whereas one observes from Figure 1 that the double-hull design tankers have oil compartments distributed over its entire length. Hence, an overall comparison of double-hull and single-hull design effectiveness would have to take into account the size of the vessels that typical tankers interacts with and at what speeds and interaction angles. Section 5 describes such an evaluation using an MTS simulation approach.

4. Construction of a grounding oil outflow model

   The approach towards developing an oil outflow model for grounding scenarios is analogous to the approach for the collision scenarios outlined in Figure 2. Figure 11 provides an overview of the different analysis steps for the grounding oil outflow model. Comparing Figure 11 and Figure 2, one observes that a polynomial regression and a binary logistic regression also provide the coefficients for Step 1 and Step 2 calculations in Figure 11. The data analysis procedure is similar to that described in Sections 3.1 and 3.2. Complete details are provided in van de Wiel (2008). Below we shall describe some nuanced difference between the construction of the grounding oil outflow model and the collision oil outflow model.

   Of course, in the case of grounding one does not have to take into account an interacting vessel in the outflow model, and a tanker's displacement and speed are directly transformed into a kinetic energy predictor variable. A difference between the grounding scenario data and the collision scenario data in the SR259 report is that grounding scenarios provide a longitudinal damage start y_{l_1} and y_{l_2}, whereas the collision scenario data only provide longitudinal damage y_l. This prompted the third simulation data analysis step "Damage Location Analysis" in case of collisions depicted in Figure 2 and described in Section 3.3. Hence, this step is omitted from Figure 11. Moreover, in 98.5% of the SH cases and in 94% of the DH cases the value of y_{l_1} equals zero, indicating that longitudinal damage extent in most cases starts at the bow. Hence, we make the simplifying worst case assumption that y_{l_1} equals zero in our oil outflow model and y_{l_2} is estimated via a polynomial regression analysis.
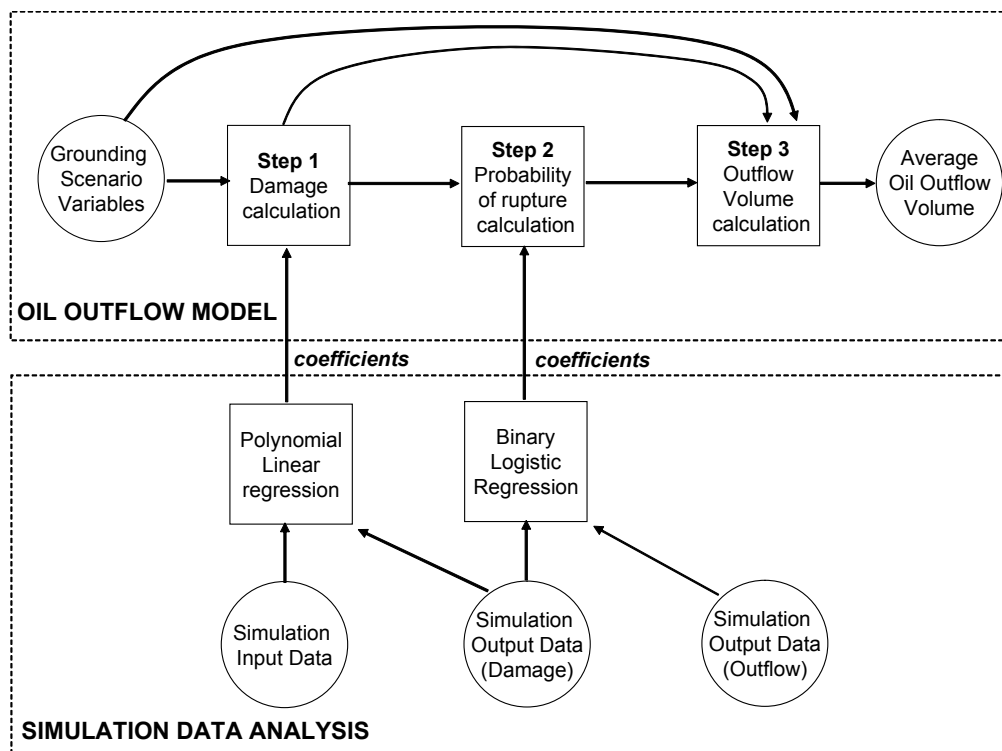
**Figure 11. Grounding modeling overview**

The grounding damage extent output data contains a vertical damage extent y_v which equals the penetration depth of the rock into the tanker. This is evaluated in the SR259 report directly from the tanker's draft and the obstruction depth of the rock itself in a particular grounding accident scenario. No information is provided in the SR259 report regarding the distribution of the transversal damage extent y_t across the impact location c (measured relatively over the width of the tanker in this case). Hence, we shall assume that transversal damage y_t is symmetrically distributed across impact location c.

While the outflow volume evaluation in the SR259 report used a hydrostatic balance analysis (allowing some oil to remain within a tank compartment), we make for consistency of comparison between the grounding and collision oil outflow models the worst case assumption that all oil of a penetrated compartment is lost. Hence, similar to the collision models, we utilized a tanker's compartment design and combined it with damage extents y_l, y_t and y_v and evaluated the overall oil carrying capacity z of damaged compartments. As before in Section 3, we next evaluate an average oil outflow for this grounding accident scenario by weighing z with the probability of tank rupture evaluated using binary logistic regression analysis coefficients.

5. Analysis of double-hull versus single-hull effectiveness within a geographic context

In this section we shall present an analysis of the overall effectiveness of double-hull tankers versus single-hull tanker designs in a maritime transportation system (MTS) simulation study with oil transportation routes traversing through the San Juan Islands in Washington State. The geographic area is delineated by the blue line segments in Figure 13. For a description of this area see, e.g., Evans et al. (2001). The oil outflow model described in this paper serves in that geographic context as the final analysis layer for a causal chain analysis as depicted in Figure 12. The causal chain modeling and analysis procedure is described in detail in van Dorp et al. (2001) and Merrick et al. (2002). Recent advances in this methodology are summarized in van Dorp and Merrick (2009).
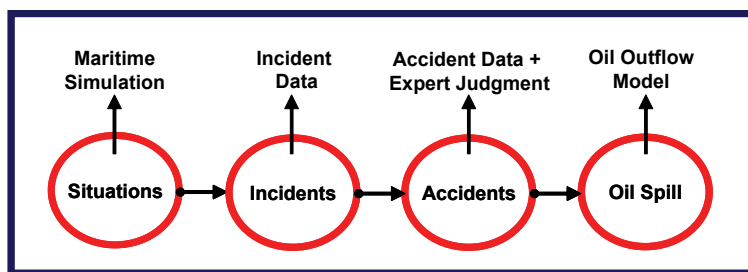
Figure 12. Causal chain of events interconnected by causal pathways.

The vessel of interests (VOI's) shall be tankers, articulated tug barges (ATB's) and integrated tug barges (ITB's) which transport both crude oil and refined products throughout the study area. The approximate locations of Refineries 1 and 2 (5 and 6) are located towards the north (the south), see Figure 13. The approximate location of Refineries 3 and 4 are indicated in Figure 13 as well. Of Refineries 5 and 6, one has not refined since 1998 and its facility currently serve as a petroleum product tank farm. The northerly route (through Rosario Strait) towards Refineries 1 and 2 is classified as a one way zone for certain larger vessels. An escorting regime for escorting laden tank vessels was implemented in the MTS simulation that mimics the current escorting operations within this geographic study area. We shall consider two causal chain analysis scenarios. In Scenario 1 all VOI's are assumed to have a single-hull design and in Scenario 2 we shall assume that all VOI's have a double-hull design. The typical tanker designs of the SR259 report (NRC, 2001) were selected to represent a VOI based on its length and width. Displacement is a driving factor in the evaluation of longitudinal kinetic energy $e_{k,p}$ and tangential kinetic energy $e_{k,t}$ as defined by equation (4). Hence, the selected VOI tanker designs were sized to conform with the VOI's dimensions. Moreover, VOI tank capacities were rescaled and a VOI's displacement was evaluated as a function of its cargo load.

Oil losses are classified in two categories designated VOI PO and VOI NPO. The VOI PO category are those oil losses from VOI's that originate from either crude cargo or bunker fuel compartments. The crude cargo and bunker fuel are called persistent oil (PO) since they are

"heavier" and less volatile then refined products and diesel fuel. Refined products and diesel fuel are referred to as non-persistent oil (NPO). Thus the category VOI NPO refers to the non-persistent oil losses from VOI compartments. Table 10 provides the total annual average oil outflow in cubic meters by accident type and by the two oil spill categories VOI PO and VOI NPO for both the single-hull and double-hull MTS simulation scenarios.

From Table 10 we observe approximately a $100\% - 25.6\% = 74.4\%$ reduction in total average annual oil outflow from the single-hull scenario ($1365.3\,m^3$) to the double-hull scenario ($349.4m^3$). A reduction by about a factor of 4. Moreover, we observe from Table 10 a reduction of $100\% - 49.4\% = 51.6\%$ in overall collision oil outflow going from single-hull to double-hull and $100\% - 20.3\% = 79.7\%$ in groundings. Thus considering that imposing a double-hull requirement on tankers was envisioned as a risk intervention measure for grounding accidents, one observes that it is evidently effective. Overall, a similar conclusion of risk reduction effectiveness of the double-hull requirement applies to collisions as well. Finally, observe from Table 10 that in both the single and double-hull MTS simulation scenarios the VOI PO category is evaluated as the larger one compared to the VOI NPO category.
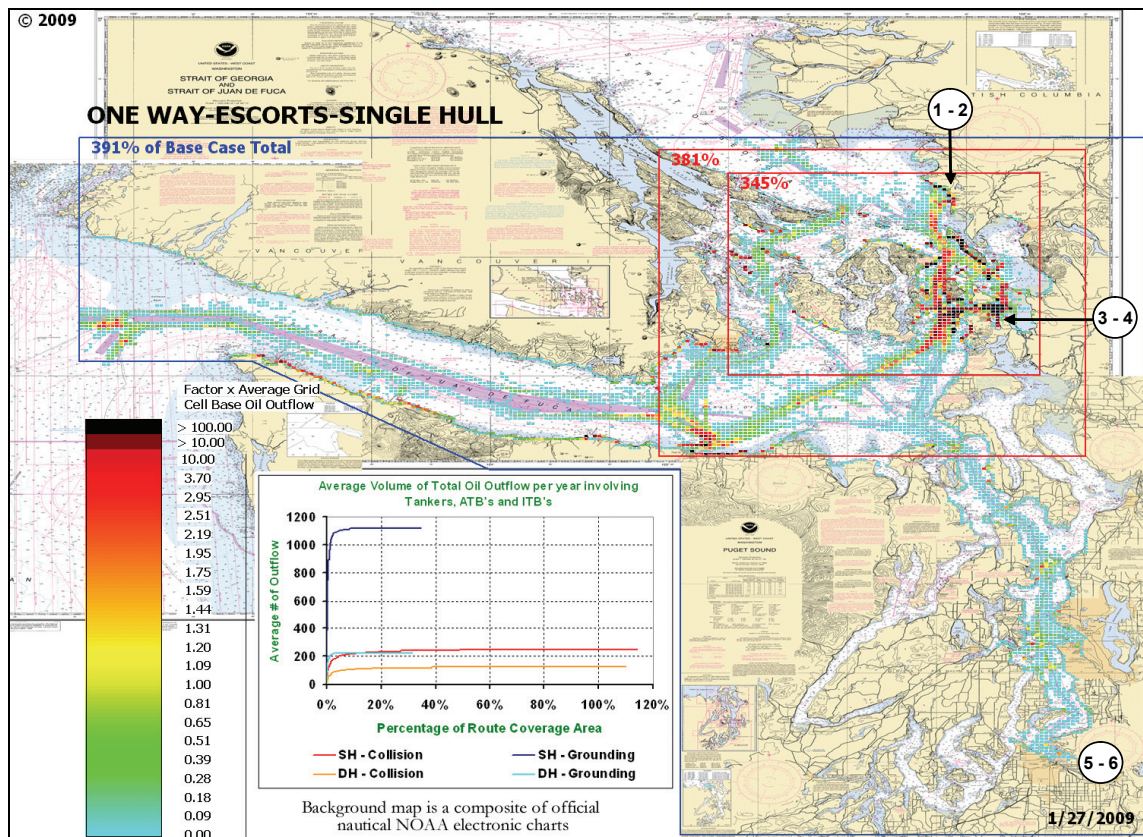

Figure 13. Geographic oil outflow profile of single-hull case.

Table 10. Summary analysis results of single-hull and

double-hull comparison in a geographic context.

A: SINGLE HULL (in cubic meters)	VOI PO	VOI NPO	Total Outflow
Collisions	222.7	24.8	247.5
Groundings	1042.3	75.4	1117.8
Total Outflow	1265.1	100.2	1365.3
B: DOUBLE HULL (in cubic meters)	**VOI PO**	**VOI NPO**	**Total Outflow**
Collisions	109.8	12.4	122.2
Groundings	217.0	10.3	227.3
Total Outflow	326.8	22.6	349.4
C: % CHANGE FROM DOUBLE HULL	**VOI PO**	**VOI NPO**	**Total Outflow**
Collisions	202.8%	200.5%	202.6%
Groundings	480.3%	735.5%	491.9%
Total Outflow	387.1%	443.2%	390.7%
D: % CHANGE FROM SINGLE HULL	**VOI PO**	**VOI NPO**	**Total Outflow**
Collisions	49.3%	49.9%	49.4%
Groundings	20.8%	13.6%	20.3%
Total Outflow	25.8%	22.6%	25.6%

Please observe that Table 10 indicates a larger percentage of the total average oil outflow due to groundings than collisions. A detailed historical analysis of accident records from 1995-2005 for the study area resulted in one collision and one grounding over that time frame for its VOI category. Thus, the MTS simulation was calibrated to predict on average the same frequency of collisions and grounding accidents. Combining that information with the fact that either the tanker or the other vessel involved in a collision is the one who gets hit, it is perhaps not surprising that our model evaluates a higher oil outflow due to groundings as opposed to collisions. (Recall the no-outflow assumptions when the tanker strikes.) Remaining drivers for the difference in average oil outflow due to collisions and groundings are e.g., traffic distribution, congestion of waterways and typical cargo loads as VOI's traverse the study area.

5.1. A geographic distribution of aggregate oil outflow analysis results

While the analysis in Table 10 allows for an aggregate effectiveness evaluation of the double-hull risk intervention measure over a defined study area, it does not provide information of the distribution of the average oil outflow analysis results across the study area. Figure 13 further displays the distribution of the combined annual average oil outflow in the single-hull case in a geographic oil outflow profile. Oil outflow losses by location and size are explained through the use of a color scale. Those grid cells within Figure 13 that have a higher oil outflow receive a darker color than those that have less oil outflow, according to the color legend. This geographic profile

format was used in Merrick et al. (2003) to display traffic congestion. It has been enhanced to also display distributed average oil outflow results.

A non-linear color legend scale is defined in Figure 13 such that the beginning of the yellow color range (the color next to the number 1.00) coincides with the oil outflow loss averaged over all grid cells that experience losses. Hence, those grid cells that have a color from the yellow color on and upward along the color scale in Figure 13, exhibit a larger than average oil outflows and those grid cells with a green color and light blue color exhibit a smaller than average oil outflow. Thus we observe from Figure 13 the larger average oil outflows closer to the locations of Refineries 1-4 than Refineries 5-6. While Figure 13 displays an aggregated oil outflow distribution, separate geographic profiles can be generated for both VOI PO and VOI NPO oil loss categories in Table 10.

Shifting our attention to the plot in the middle of the geographic profile one observes a further indication that the distribution of outflow across grid cells is non-linear. The horizontal axis list the percentage of grid cells in Figure 13 that have color (and thus potentially experience oil outflow), whereas the vertical axis displays oil outflow volume (in m^3). The curves in this plot display the progression in the cumulative oil outflow by accident type and MTS simulation scenario when ordering the grid cells by their average oil flow from largest to smallest. Focusing on the end points of these curves we arrive at the same conclusion previously derived from Table 10, i.e. the analysis results herein indicate a larger average oil outflow due to groundings than collisions.

Percentages along the x-axis in these plots are measured relative to the total annual number of grid cells that VOI's traverse through. The grid cells with color that result from collisions interaction, color both the grid cell location of the VOI and the interaction vessel (van Dorp and Merrick, 2009). Hence, the coverage area of collisions naturally covers a larger area than the route coverage alone of VOI's and hence its end-point along the x-axis goes beyond the 100% value. We conclude from the collison plots in Figure 13 that the top 60% (being conservative) of the collision interaction grid cells account for almost all of the average oil outflow loss due to collisions. Please note that the coverage area of groundings just exceeds 30% along the same x-axis. One observes a larger non-linearity for the grounding curves than the collision curves which combined with the smaller coverage areas indicates a higher concentration of oil flow results, i.e. larger average oil outflows distributed over fewer grid cells.

A similar behavior may be observed from the colors in the geographic profiles which shows a relative small coverage of darker colors (yellow and above) and a larger area of light colors (blue and green), but also follows from the displayed percentages in top left corners of the border areas in Figure 13. The 391% in the top left corner of the blue bordered area coincides with the 390.7% displayed in the lower right corner of Sub-Table C in Table 10. Hence, observe from Table 10 that this percentage is measured relative to the total average oil outflow of the double-hull MTS simulation scenario. Analagously, we observe 381% oil outflow in the upper left corner of the larger

red rectangle and 345% in the smaller one. We thus conclude from Figure 13 that about $381\%/391\% \approx 97\%$ of the average total oil outflow in the single-hull scenario occurs within the larger red rectangle in Figure 13 and $345\%/391\% \approx 88\%$ in the smaller one. Consequenty, about $97\% - 88\% \approx 11\%$ of the total average outflows falls outside the smaller red rectangle but inside the larger one, with a high concentration being observed in its lower left corner. This happens to be the area where deep draft vessel "dip" downwards to pick up pilots to continue their journey.

6. Concluding Remarks

The oil outflow model in this paper was specifically constructed to serve as an analysis layer of a causal chain analysis (depicted in Figure 12) where an MTS simulation generates accident scenarios. A one year run of this MTS simulation for the analysis in Section 5 generates over $150,000$ collision scenarios and $1,200,000$ grounding scenarios. This amounts to over 17 times the $80,000$ accident scenarios generated for the SR259 report, which reemphasizes the need for a computationally efficient oil outflow analysis layer. The oil outflow model herein does not provide an alternative to the physical damage simulation software SIMCOL or DAMAGE described in more detail in the introduction. These tools are more geared towards evaluating detailed naval architectural design changes at the ship level rather than an aggregate geographic oil outflow profile analysis (see, e.g, Figure 13).

The MTS risk simulation set-up allows one to analyze other what-if scenarios besides the double-hull/single-hull analysis presented in Section 5. For example, van Dorp and Merrick (2009) look back further in time and investigate MTS simulation scenarios where two-way traffic is allowed in the north-south bound direction for certain larger vessels in the smaller red rectangle in Figure 13 and no-escorting is provided in the larger one. Besides offering a retrospective analysis of risk interventions currently in place, the MTS risk simulation combined with the oil outflow analysis layer also offers a prospective analysis tool of risk interventions that are being considered, such as e.g. traffic procedure changes in navigation channels or expanding escorting across a larger area. In our opinion, relative comparisons of analysis scenarios of this nature across accident types, oil outflow categories, and various risk interventions ought to be emphasized, while concentrating less on the absolute values of the analyses results in these what-if scenarios.

Acknowledgements

References

Bookrags (2009). Mallows' cp summary. http://www.bookrags.com/wiki/Mallows

Brown, A (2001). *Alternative Tanker Designs, Collision Analysis.* NRC Marine Board Committee on Evaluating Double-Hull Tanker Design Alternatives.

Brown, AJ, and Amrozowicz, M (1996). Tanker environmental risk - putting the pieces together. *Joint SNAME/SNAJ Conference on Designs and Methodologies for Collision and Grounding Protection of Ships*, San Francisco, CA.

Chen, D (2000). *Simplified Collision Model (SIMCOL)*, M.S. thesis. Virginia Tech, Blacksburg, May.

Crake, K (1995). *Probabilistic Evaluations of Tanker Ship Damage in Grounding Events*, Naval engineer thesis. Massachusetts Institute of Technology, Cambridge.

Draper, N and Smith, H (1998). *Applied Regression Analysis.* Wiley, The Netherlands.

Evans DL, Grudes SB, Davidson, MA (2001). *United States Coast Pilot, Pacific Coast, California, Oregon, Washington and Hawai, Vol. 7*, National Ocean Service, U.S. Department of Commerce, Washington D.C.

Hosmer, D, and Lemeshow, S (2002). *Applied Logistic Regression.* Second Edition. Wiley-Interscience.

Huijer, K (2005) Trends in oil spills from tanker ships, 1995-2004. London.

International Maritime Organization (1995). I*nterim guidelines for the approval of alternative methods of design and construction of oil tankers under regulation 13f(5) of annex i of marpol 73/78.*

Merrick JRW, van Dorp JR, Harrald J, Mazzuchi T, Spahn J, Grabowski M (2002). The Prince William Sound Risk Assessment. *Interfaces,* 32 (6), 25-40.

Merrick JRW, van Dorp JR, Blackford JP, Shaw GL, Mazzuchi TA and Harrald JR (2003). A Traffic Density Analysis of Proposed Ferry Service Expansion in San Francisco Bay Using a Maritime Simulation Model, *Reliability Engineering and System Safety*, 81 (2), 119-132.

Minorsky, V (1959). An analysis of ship collisions with reference to protection of nuclear power plants. *Journal of Ship Research* 3, 1.

National Research Council (2001). *Environmental Performance of Tanker Designs in Collision and Grounding,* Special Report 259, The National Academies Press.

Rawson, C, Crake, K and Brown, AJ (1998), Assessing the Environmental Performance of Tankers in Accidental Grounding and Collision, *SNAME Transactions* 106, 41-58

Rodrigue, JP, Comtois, C, and Slack, B (2006). *The Geography of Transport Systems.* Routledge, New York.

Schmeiser, B (1999). Advanced input modeling for simulation experimentation. *Proceedings of the 1999 Winter Simulation Conference*, 110-115.

Simonsen, BC (1998). *DAMAGE Theory Validation. Report 63.* Joint MIT-Industry Program on Tanker Safety, May.

Simonsen, BC and Wierzbicki, T (1996). *Theoretical Manual on Grounding Damage of Hull Bottom Structure, Volume II. Report 55.* Joint MIT-Industry Program on Tanker Safety.

Simonsen, BC and Wierzbicki, T (1997). *Theoretical Manual on Grounding Damage of Ships, Volume III. Report 59.* Joint MIT-Industry Program on Tanker Safety, June.

Tikka, K (2001). *Alternative Tanker Designs, Grounding Analysis.* NRC Marine Board Committee on Evaluating Double-Hull Tanker Design Alternatives.

UNCTAD (2007). *Review of maritime transport 2007.* New York, Geneva.

US Coast Guard (2008). *Incident Specific Preparedness Review (ISPR) M/V Cosco Busan Oil Spill in San Francisco Bay,* Accessed January 2009, http://uscg.mil/foia/CoscoBuscan/ CoscoBusanISPRFinal.pdf

van de Wiel, G (2008). A Probabilistic Model for Oil Spill Volume in Tanker Collisions and Groundings. Delft University of Technology, 2008.

van der Laan, M (1997). *Environmental Tanker Design.* Delft University of Technology, 1997.

van Dorp JR, Merrick J, Harrald J, Mazzuchi T, Grabowski M (2001). A Risk Management Procedure for the Washington State Ferries, *Risk Analysis*, 21 127-142.

van Dorp JR, Merrick JRW (2009). On a Risk Management Analysis of Oil Spill Risk using Maritime Transportation System Simulation, To appear in the Special Volume on Port Security/Safety, Risk Analysis and Modeling in *Annals of Operations Research.*